Front. Optoelectron. 2012, 5(2): 218–223
DOI 10.1007/s12200-012-0233-6

RESEARCH ARTICLE

Measurement of optical mirror with a small-aperture interferometer

Ya GAO[1], Hon Yuen TAM[2], Yongfu WEN[1], Huijing ZHANG[1], Haobo CHENG (✉)[1]

1 School of Optoelectronics, Beijing Institute of Technology, Beijing 100081, China
2 Department of Manufacturing Engineering and Engineering Management, City University of Hong Kong, Hong Kong, China

Abstract In this paper, the principle of subaperture stitching interferometry was introduced. A testing stage with five degrees of freedom for stitching interferometry was built. A model based on least-squares method and error averaging method for data processing was established, which could reduce error accumulation and improve the precision. A 100 mm plane mirror was measured with a 50 mm aperture interferometer by means of stitching interferometry. Compared with the results by a 100 mm interferometer, peak to valley (PV) and root mean square (RMS) of the phase distribution residual are 0.0038λ and 0.0004λ, respectively. It proved that the model and method are helpful for large optical measurement.

Keywords subaperture stitching, interferometry, residual error

1 Introduction

Optical testing technology is important for optical manufacturing [1]. Interferometry is widely used to test optical elements [2]. Usually large aperture sample has to be measured by an interferometer with auxiliary components. For example, autocollimation method needs a standard reference plane mirror which has same size as the sample; computer generated hologram method requires the production of holographic panels [3]. Manufacture of auxiliary components is difficult and costly, so it does not have universal application. Subaperture stitching method can test large diameter optical components with small diameter interferometer which does not require auxiliary components [4].

Kim of Arizona in US first proposed the principle of stitching interferometry in the 1980s. He tested a parabolic mirror by means of autocollimation with small diameter flat mirror array instead of large diameter flat mirror [5]. And Chow and Lawrence presented a method to stitch subaperture simultaneously by Zernike polynomials fitting algorithm [6]. Then, Hainaut and Erteza used filter techniques for the data processing of stitching interferometry [7]. Moreover, Catanzaro et al. tested the 3.5 m telescope of Herschel Space by means of stitching interferometry in 2001 [8]. In 2004, David Redding tested James Webb Space Telescope system.

In China, research of subaperture stitching interferometer technology began in the 1990s, now there are several laboratories working on this field. But there are few reports about testing and error analysis of large diameter plane mirror yet.

A testing stage with five degrees of freedom was built. A 100 mm aperture mirror was tested with a 50 mm aperture interferometer by means of subaperture stitching interferometry. Measurements of subapertures were connected by means of least-squares and error averaging method. The mirror was tested with a 100 mm aperture interferometer. The residual error is in the tolerance of equipment.

2 Principles

2.1 Principles of stitching interferometry

The way of subaperture stitching interferometry is that to measure the glass part by part with a small-aperture interferometer and connect the measurements together. However, these measurements cannot be connected directly because of some errors such as tilt and shift. When the adjacent measurements are made so that they have common area, they can be connected by minimizing the error of the phase distributions in the common area.

Two adjacent areas named Φ and Φ' are taken for example, as shown in Fig. 1. They are measured with a shift (x_0, y_0), and the phase distributions are expressed as

Received December 1, 2011; accepted December 8, 2011

E-mail: chenghaobo@tsinghua.org.cn

$\Phi(x,y)$ and $\Phi'(x',y')$ separately. The coordinates of (x',y') shifts from (x,y) by following relations:

$$\begin{cases} x = x' + x_0, \\ y = y' + y_0. \end{cases} \tag{1}$$

If the coordinate and the phase distribution in the area of Φ are set as a standard, two phase distributions can be expressed as $\Phi(x,y)$ and $\Phi'(x-x_0,y-y_0)$ separately. In the common area, the relation of Φ and Φ' fulfills the following equation:

$$\Phi(x,y) = \Phi'(x-x_0,y-y_0) + ax + by + c, \tag{2}$$

where a and b are coefficients of the tilt of the sample in the x and y directions, respectively; and c is a constant phase shift due to the vertical movement of the sample.

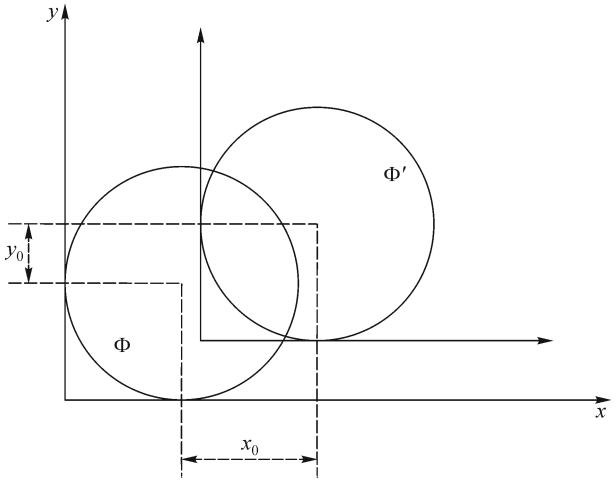

Fig. 1 Illustration of principle

The least-squares method is used to find the coefficients, in which the sum of the squared difference of the phase distributions in the common area is minimized,

$$\sum \{\Phi(x,y) - [\Phi'(x-x_0,y-y_0) + ax + by + c]\}^2 \rightarrow \min, \tag{3}$$

if n is the number of the sampling points in the common area, the summation can be expressed as following:

$$\sum_n \{\Phi(x,y) - [\Phi'(x-x_0,y-y_0) + ax + by + c]\}^2 \rightarrow \min, \tag{4}$$

the following matrix equation can be obtained:

$$\begin{bmatrix} \sum x\Delta(x,y) \\ \sum y\Delta(x,y) \\ \sum \Delta(x,y) \end{bmatrix} = \begin{bmatrix} \sum x^2 & \sum xy & \sum x \\ \sum xy & \sum y^2 & \sum y \\ \sum x & \sum y & n \end{bmatrix} \begin{bmatrix} a \\ b \\ c \end{bmatrix}, \tag{5}$$

where $\Delta(x,y) = \Phi(x,y) - \Phi'(x-x_0,y-y_0)$. The coefficients can be obtained as follows:

$$\boldsymbol{R} = \begin{bmatrix} a \\ b \\ c \end{bmatrix} = \begin{bmatrix} \sum x^2 & \sum xy & \sum x \\ \sum xy & \sum y^2 & \sum y \\ \sum x & \sum y & n \end{bmatrix}^{-1} \begin{bmatrix} \sum x\Delta(x,y) \\ \sum y\Delta(x,y) \\ \sum \Delta(x,y) \end{bmatrix}, \tag{6}$$

the two individual measurements Φ and Φ' can be aligned to get the entire shape of the sample after correcting tilt and vertical displacement.

2.2 Method of error averaging

If there are more than two areas, the areas can be connected one by one. But errors will be brought in and accumulated during the process. Error averaging method can be used, which minimize the sum of squared differences for all common areas simultaneously. Φ_m of M areas is set as a standard, i.e.,

$$\begin{aligned} &\Phi_m(x,y) \\ &\quad = \Phi_0(x-x_0,y-y_0) + a_0x + b_0y + c_0 \\ &\quad = \Phi_1(x-x_1,y-y_1) + a_1x + b_1y + c_1 \\ &\quad = \cdots \\ &\quad = \Phi_{m-1}(x-x_{m-1},y-y_{m-1}) + a_{m-1}x + b_{m-1}y + c_{m-1} \\ &\quad = \Phi_{m+1}(x-x_{m+1},y-y_{m+1}) + a_{m+1}x + b_{m+1}y + c_{m+1} \\ &\quad = \cdots \\ &\quad = \Phi_{M-1}(x-x_{M-1},y-y_{M-1}) + a_{M-1}x + b_{M-1}y + c_{M-1}. \end{aligned} \tag{7}$$

By using least-squares equation and error averaging method, the sum of the squared differences in the common areas is shown as following:

$$\begin{aligned} &\sum_0 \{\Phi(x,y) - [\Phi_0(x-x_0,y-y_0) + a_0x + b_0y + c_0]\}^2 \\ &+ \sum_1 \{\Phi(x,y) - [\Phi_1(x-x_1,y-y_1) + a_1x + b_1y + c_1]\}^2 \\ &+ \cdots + \sum_{m-1} \{\Phi(x,y) - [\Phi_{m-1}(x-x_{m-1},y-y_{m-1}) \\ &+ a_{m-1}x + b_{m-1}y + c_{m-1}]\}^2 + \sum_{m+1} \{\Phi(x,y) \\ &- [\Phi_{m+1}(x-x_{m+1},y-y_{m+1}) + a_{m+1}x + b_{m+1}y + c_{m+1}]\}^2 \\ &+ \cdots + \sum_{M-1} \{\Phi(x,y) - [\Phi_{M-1}(x-x_{M-1},y-y_{M-1}) \\ &+ a_{M-1}x + b_{M-1}y + c_{M-1}]\}^2 \rightarrow \min, \end{aligned} \tag{8}$$

where a_i, b_i, and $c_i (i = 0,1,...,m-1,m+1,...,M)$ are coefficients of every area respectively. If $\Delta(x,y) = \Phi_i(x_i,y_i) - \Phi_j(x_j,y_j)$, and $\boldsymbol{P}$, $\boldsymbol{Q}$, $\boldsymbol{R}$ is given by

$$\boldsymbol{P}_{ij} = \begin{bmatrix} \sum_{i\cap j} x\Delta(x,y) \\ \sum_{i\cap j} y\Delta(x,y) \\ \sum_{i\cap j} \Delta(x,y) \end{bmatrix}, \quad \boldsymbol{Q}_{ij} = \begin{bmatrix} \sum_{i\cap j} x^2 & \sum_{i\cap j} xy & \sum_{i\cap j} x \\ \sum_{i\cap j} xy & \sum_{i\cap j} y^2 & \sum_{i\cap j} y \\ \sum_{i\cap j} x & \sum_{i\cap j} y & n_{ij} \end{bmatrix},$$

$$\boldsymbol{Q}_{ii} = \begin{bmatrix} 0 & 0 & 0 \\ 0 & 0 & 0 \\ 0 & 0 & 0 \end{bmatrix}, \quad \boldsymbol{R}_i = \begin{bmatrix} a_i \\ b_i \\ c_i \end{bmatrix}, \tag{9}$$

where n_{ij} is the number of sampling points in the common area of Φ_i and Φ_j, if there is no common area between Φ_i and Φ_j, $\boldsymbol{P}_{ij}$ and $\boldsymbol{Q}_{ij}$ become null matrix, the following matrix can be obtained:

$$\left[\left(\sum_k^{M-1} P_{ik}\right)_i\right] = \left[\left(Q_{ij} - \delta_{ij}\sum_k^{M-1} Q_{ik}\right)_{ij}\right][(R_i)_i], \tag{10}$$

where $i,j = 0,1,...,m-1,m+1,...,M$; $k = 0,1,...,M$, and δ_{ij}, $\sum_k^{M-1} P_{ik}$ and $\sum_k^{M-1} Q_{ik}$ obey the relation:

$$\delta_{ij} = \begin{cases} 1, & \text{if } i = j, \\ 0, & \text{if } i \neq j, \end{cases}$$

$$\sum_k^{M-1} P_{ik} = P_{i0} + P_{i1} + \cdots + P_{iM-1},$$

$$\sum_k^{M-1} Q_{ik} = Q_{i0} + Q_{i1} + \cdots + Q_{iM-1}. \tag{11}$$

The full aperture shape of the sample can be obtained by aligning all measurements [9–11].

2.3 Tilt error

Tilt error will be brought during measurement and accumulated in data process, which should be deleted to improve precision. Method of phase data fitting for Zernike polynomials can be used. The Zernike polynomials are represented as follows:

$$\sum_{n=1}^{N} a_n Z_n(x_i,y_i) = \Phi(x_i,y_i). \tag{12}$$

If M points are gotten for sample, there will be

$$\sum_{i=1}^{M}\left(\sum_{n=1}^{N} a_n Z_n(x_i,y_i) - \Phi(x_i,y_i)\right) \rightarrow \min, \tag{13}$$

where N is the number of polynomial item, a_n is the coefficients for the nth polynomial. So a_0, a_1 and a_2 are pistons, tilted in the x and y directions respectively. The phase distribution Φ will eliminate tilt error by subtracting the first three of Zernike polynomial [12].

3 Experiments

A testing translation stage with five-dimension was built for the experiment. The structure and appearance of the equipment are shown in Fig. 2. The stage is set up on an air-floated table. Workpiece is moved and tilted along x and y direction precisely and rotated around z direction. The precision of motion platform should be better than the spatial resolution of the interferometer to meet the requirements of the experiment because the charge coupled

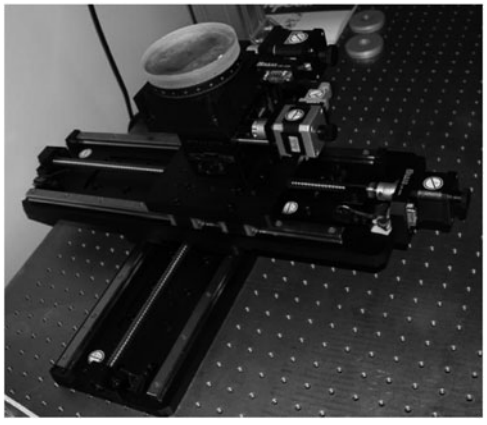

Fig. 2 Translation stage

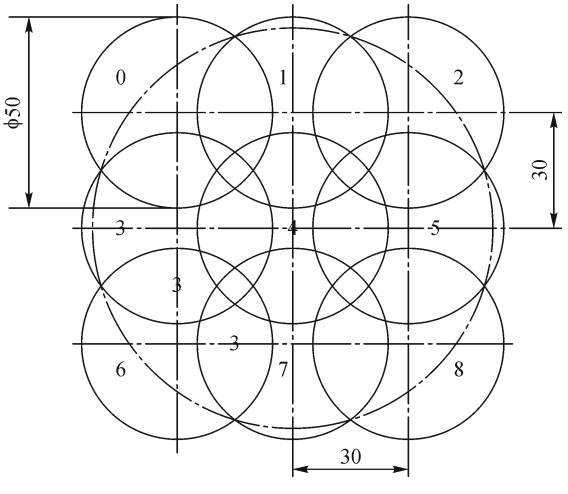

Fig. 3 Location of nine subapertures

device (CCD) of interferometer cannot distinguish the error in this case. Size of the two lens of interferometer used in the experiment are 50 and 100 mm, separately, and the effective pixels of FISBA are 1000 × 1000 pixels. So resolution of the interferometer is 0.05 mm. The positioning accuracy and linearity of x and y stages are required to be better than 0.05 mm. The precision and other parameters of the platform are given by Table 1.

A 100 mm aperture plane mirror was tested using 50 mm aperture lens by stitching interferometry. Nine sub-apertures are placed parallelly to cover the mirror, as shown in Fig. 3, and the overlapping area of adjacent sub-apertures is greater than 25% of nine subapertures.

The measurements of nine subapertures are shown in Fig. 4. The number and locations of nine subapertures are shown in Fig. 3. The number of x-axis and y-axis represent

Table 1 Stage parameters

No.	Max. stroke/mm	positioning accuracy/mm	straightness accuracy/mm
1. x-direction	300	0.02	0.02
2. y-direction	300	0.02	0.02
No.	angle range/(°)	resolution	reposition accuracy
3. x-goniometer	±10	0.00032	0.0043
4. y-goniometer	±15	0.00045	0.0047

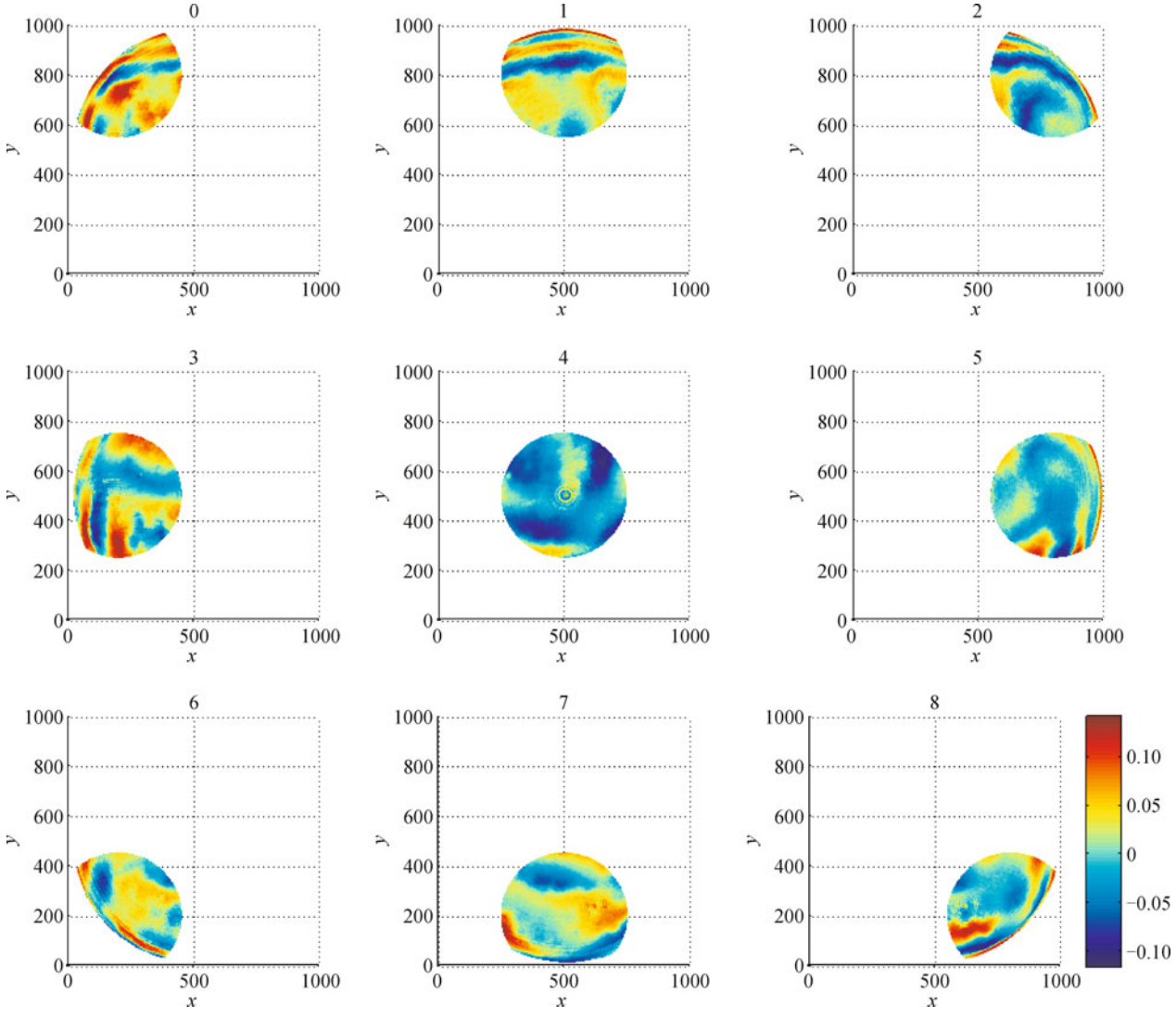

Fig. 4 Measurements of nine subapertures separately (unit: λ)

the sampling points in both directions. The unit of the color bar is λ. They are stitched together after eliminating the tilt error to get the full-aperture phase distributions, which is shown in Fig. 5(a). The result measured with the 100 mm aperture lens is shown in Fig. 5(b) for comparison.

Figure 6 shows the results of measurement, which have eliminated tilt error by means of Zernike fitting. Figure 6(a) shows the entire shape stitched. The peak to valley (PV) and root mean square (RMS) are 0.1842λ and 0.0289λ, respectively. Figure 6(b) shows the measurement of the sample with 100 mm aperture interferometer, PV = 0.1880λ and RMS = 0.0293λ ($\lambda = 632.8$ nm), respectively. Deviation are ΔPV = 0.0038λ, ΔRMS = 0.0004λ. Figure 7 shows the deviation, and mean of absolute value of deviation is 0.022λ. Tolerance of interferometer is PV = 0.02λ, RMS = 0.0004λ. The deviation is well close to the tolerance of the interferometer.

4 Conclusions

A testing stage with five degrees of freedom for stitching interferometry was built. A model based on least-squares method and error averaging method was established for data processing. A 100 mm aperture flat mirror was measured with a small aperture interferometer by means of stitching interferometry. The measurements of nine small subapertures were aligned together by minimizing the difference of the phase distributions in the common area by means of least-squares method and error averaging

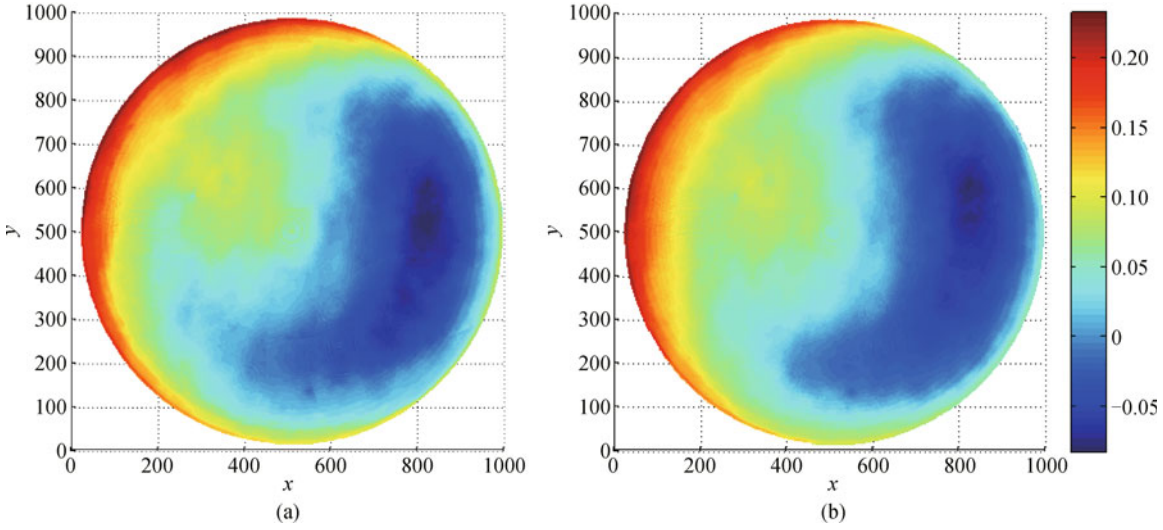

Fig. 5 Data processing results of (a) stitching; (b) measurement (unit: λ)

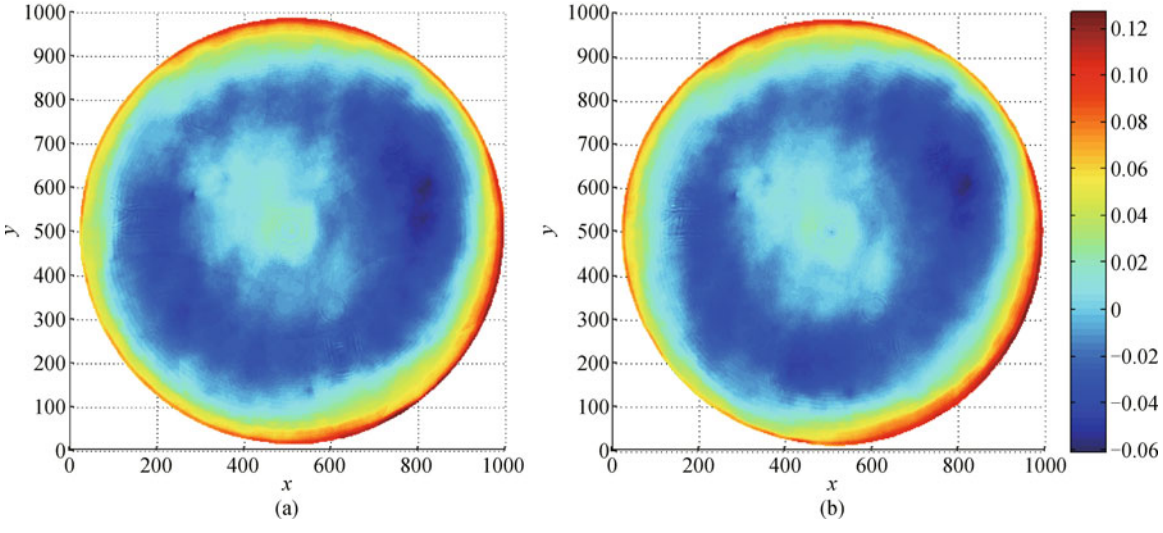

Fig. 6 Results after eliminating tilt error. (a) Stitching; (b) measurement (unit: λ)

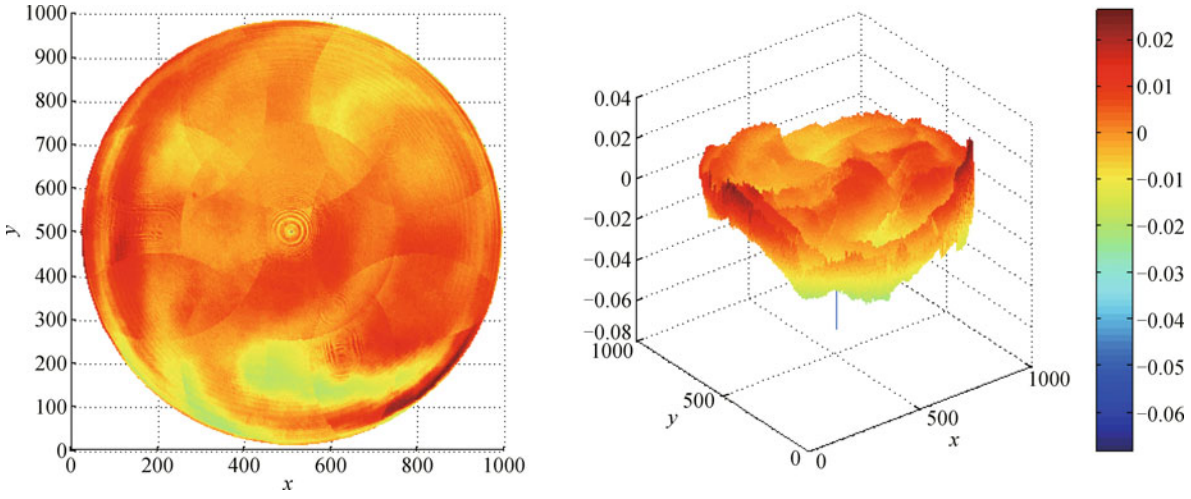

Fig. 7 Deviation (unit: λ)

method. Compared the results with the 100 mm aperture interferometer, the PV and RMS of the phase distribution residual are 0.0038λ and 0.0004λ, separately, which are in the tolerance of the interferometer. Further research will focus on large plane mirror and aspheric lens. Large plane mirror can be tested by aligning more than nine subapertures with this model. Aspheric lens should be measured by a six-dimension testing translation stage, which can change the distance between the lens and interferometer. And the defocusing error of subapertures should be correct for stitching.

Acknowledgements This work was supported by the National Natural Science Foundation of China (Grant No. 61128012) and the Research Grants Council of the Hong Kong Special Administrative Region (No. 9041577).

References

1. Cheng H B. Interferometric null testing and the model for separating adjustment errors. Journal of Harbin Institute of Technology, 2006, 38(8): 1247–1250
2. Yang L. Advanced Optical Manufacture Technology. Beijing: Science Press, 2001, 326–365 (in Chinese)
3. Malacara D. Optical Shop Testing. New York: Wiley-Interscience, 1978, 245–296
4. Cheng H B, Feng Z J. Error-separation model for interferometric testing aspheric surfaces based on wavefront aberrations. Journal of Tsinghua University (Science and Technology), 2006, 46(2): 187–190
5. Kim C J. Polynomial fit of interferograms. Applied Optics, 1982, 21 (24): 4521–4525 doi:10.1364/AO.21.004521
6. Chow W W, Lawrence G N. Method for subaperture testing interferogram reduction. Optics Letters, 1983, 8(9): 468–470
7. De Hainaut C R, Erteza A. Numerical processing of dynamic subaperture testing measurements. Applied Optics, 1986, 25(4): 503–509
8. Catanzaro B E, Connell S J, Mimovich M, Backovsky S, Williams G, Thomas J A, Barber D D, Johnston R A, Hylton J C, Dodson K J, Cohen E J. Cryogenic (70 K) measurement of an all-composite 2-meter diameter mirror. Proceedings of SPIE, the International Society for Optical Engineering, 2001, 4444: 238–255
9. Bray M. Stitching interferometer for large optics: recent developments of a system. Proceedings of SPIE, the International Society for Optical Engineering, 1999, 3492(2): 946–956
10. Bray M. Stitching interferometer for large plano optics using a standard interferometer. Proceedings of SPIE, Optical manufacturing and testing II, 1997, 3134(1): 39–50
11. Otsubo M, Okada K, Tsujiuchi J. Measurement of large plane surface shapes by connecting small-aperture interferograms. Optical Engineering, 1994, 33(2): 608–613
12. Negro J E. Subaperture optical system testing. Applied Optics, 1984, 23(12): 1921–1930